IGNITION TRANSIENTS AND PRESSURIZATION IN CLOSED CHAMBERS

Leonard H. Caveny, et al

Princeton University

Prepared for:

Ballistic Research Laboratories

November 1975

BRL MR 2558

BRL

AD

MEMORANDUM REPORT NO. 2558

IGNITION TRANSIENTS AND PRESSURIZATION IN CLOSED CHAMBERS

Leonard H. Caveny
Martin Summerfield

Princeton University
Princeton, NJ

Carl W. Nelson

Ballistic Research Laboratories

November 1975

USA BALLISTIC RESEARCH LABORATORIES
ABERDEEN PROVING GROUND, MARYLAND

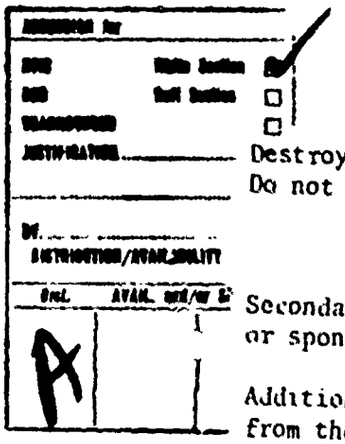

Destroy this report when it is no longer needed. Do not return it to the originator.

Secondary distribution of this report by originating or sponsoring activity is prohibited.

Additional copies of this report may be obtained from the National Technical Information Service, U.S. Department of Commerce, Springfield, Virginia 22151.

The findings in this report are not to be construed as an official Department of the Army position, unless so designated by other authorized documents.

UNCLASSIFIED

SECURITY CLASSIFICATION OF THIS PAGE (When Data Entered)

REPORT DOCUMENTATION PAGE		READ INSTRUCTIONS BEFORE COMPLETING FORM
1 REPORT NUMBER BRL MEMORANDUM REPORT NO. 2558	2 GOVT ACCESSION NO	3 RECIPIENT'S CATALOG NUMBER
4. TITLE (and Subtitle) IGNITION TRANSIENTS AND PRESSURIZATION IN CLOSED CHAMBERS		5 TYPE OF REPORT & PERIOD COVERED Technical 1 Dec 1973 - 30 Nov 1974 6 PERFORMING ORG. REPORT NUMBER
7 AUTHOR(s) Leonard H. Caveny and Martin Summerfield, Princeton University Carl W. Nelson, Ballistic Research Labs.		8 CONTRACT OR GRANT NUMBER(s) DAAD05-72-C-0135
9 PERFORMING ORGANIZATION NAME AND ADDRESS Princeton University, Princeton, NJ and USA Ballistic Research Laboratories, Aberdeen Proving Ground, MD		10 PROGRAM ELEMENT PROJECT TASK AREA & WORK UNIT NUMBERS
11 CONTROLLING OFFICE NAME AND ADDRESS US Army Materiel Command Alexandria, VA 22333		12 REPORT DATE NOVEMBER 1975 13 NUMBER OF PAGES 55
14 MONITORING AGENCY NAME & ADDRESS(if different from Controlling Office)		15 SECURITY CLASS (of this report) UNCLASSIFIED 15a DECLASSIFICATION DOWNGRADING SCHEDULE

16 DISTRIBUTION STATEMENT (of this Report)

Approved for public release; distribution unlimited.

17 DISTRIBUTION STATEMENT (of the abstract entered in Block 20, if different from Report)

18 SUPPLEMENTARY NOTES

19 KEY WORDS (Continue on reverse side if necessary and identify by block number)

Solid propellants
Gun propellants
Single base propellants
Ignition
Unsteady burning
Relative quickness

20 ABSTRACT (Continue on reverse side if necessary and identify by block number)

Pressure versus time data obtained from igniting and burning propellants in highly loaded closed chambers (loading densities between 0.1 and 0.3 g/cm^3) are being used to evaluate propellants in empirical quality and production control procedures. Interpretations obtained from such production control devices are hampered by uncertainties concerning ignition delays, dynamic burning, heat loss, propellant surface area versus distance burned, and real gas effects. In this study, attention is focused on devising a closed chamber experiment for measuring dynamic burning rates and on developing a comprehensive analytical model of the

DD FORM 1 JAN 73 1473 EDITION OF 1 NOV 65 IS OBSOLETE

UNCLASSIFIED

SECURITY CLASSIFICATION OF THIS PAGE (When Data Entered)

20. Abstract - continued

experiment. Features of the model include the energy equation, heat-up to ignition, generalized real gas effects, and dynamic burning. Calculated results lead to improved methods for analyzing and reporting closed chamber results so as to include information on the dynamic processes that dominate ignition and the early stages of pressurization.

TABLE OF CONTENTS

LIST OF TABLE CAPTIONS

LIST OF FIGURE CAPTIONS

INTRODUCTION

Tests in which propellant granules are ignited and burned in closed chambers are used empirically as part of routine quality and production control procedures (to determine propellant acceptability, to establish charge weights, and to make laboratory determinations of propellant characteristics).[1-3] Closed chamber experiments of interest in this study use high loading of nitrocellulose based propellant (e.g., 0.1 to 0.3 g/cm^3) which produce high pressurization rates [$(dp/dt)_{max}$ of 10^4 MPa/sec and greater] and high pressures (e.g., 100 to 300 MPa). In this study, we focused our attention on closed chamber experiments as a means of learning more about dynamic burning and dynamic chamber responses that accompany ignition and rapid pressurization.

The reader should make the distinction between two very different situations in which dynamic burning and dynamic chamber responses are of interest:

1. Production Control - In operational systems in which the pressurization processes are uniform and performance is not abnormally sensitive to the propellant variations that occur during production, relative changes in dp/dt vs p (usually during the middle 40 to 80% of the pressure range) may provide sufficient information to establish the charge weight for each production propellant lot. However, further improvements of muzzle velocity predictions based on closed chamber results require a more complete understanding and interpretation of closed chamber processes.
2. Research and Development - In developmental systems (e.g., where maximum volumetric loading or optimized simulation igniters are sought), careful attention must be given to the dynamic chamber and burning responses associated with ignition and initial pressurization. In these cases, it is necessary to glean ignition, dynamic burning, and chamber dynamics information from specially devised closed chamber experiments. Thus, emphasis is given to the initial portion of the p vs t trace.

Recently, attention is being focused on specific situations which would benefit from improved understanding of how propellant variations affect closed chamber processes, e.g., Ref. 1 is directed at methods of predicting charge weights for production systems and Ref. 4 related nonuniform pressure gradients to overpressure failures and abnormal muzzle velocity and range dispersions.

While the component processes that occur in closed chamber experiments are reasonably well understood, none of the existing analytical models provide a comprehensive explanation of the interplays among these component processes. For example, uncertainties exist concerning the contributions of dynamic burning, real gas effects and the use of simple equations of state, heat losses from the gases to the chamber, variations of flame and chamber temperatures, and nonuniform ignition and surface regression of granular propellant charges.

For the most part, previous efforts considered the middle of the burning interval to avoid complications associated with the above stated uncertainties. Approaches which do not treat adequately the ignition and early pressurization phases ignore much of the information available from closed chamber experiments.

By understanding the dynamic responses in the ignition and early pressurization phases, important insights into the instabilities and oscillations that have been associated with malfunctions in operational systems (4) can be obtained. In particular, the goals of the study are:

1. To develop ignition and dynamic burning rate relationships that can be used readily in interior ballistic codes,

2. To provide an analytical basis for developing an improved method of measuring dynamic responses of propellants at high pressures and high pressurization rates, and

3. To develop a more complete model of the interactions between ignition, dynamic burning, chamber pressurization, heat loss, etc.

DESCRIPTION OF CLOSED CHAMBER

Closed chambers are usually designed to burn granular propellant charges. Several characteristics of these devices complicate the data interpretation:

1. Granular propellants are usually ignited by an unevenly dispersed secondary solid propellant charge and, thus, uncertainties exist concerning the uniformity of ignition and flame spreading.

2. Heat loss from the combustion gases to the chamber walls.

3. Burning surface area versus distance burned is altered by nonuniform ignition (and thus nonuniform surface regression) and variations in the multi-perforated grain geometry.

4. Ignition charges usually produce gas compositions and temperatures that differ significantly from those of the main charge.

For experimental determinations of batch-to-batch acceptability during propellant production, the above four complications may not be objectionable since unacceptable propellant can be isolated and charge weight determined in terms of relative changes in the pressure versus time trace. However, the complications completely mask changes in burning rate, and in particular, the dynamic responses that occur during ignition and the early phases of chamber pressurization.

We propose a special purpose closed-chamber and propellant configuration which is suited for establishing the contributions of dynamic burning and chamber responses. As shown in Fig. 1, the propellant charge consists of thin sheets of propellant bonded to the inner wall of the cylindrical chamber and to the outer diameter of the cylindrical spacer. For this simple geometry, the surface area versus distance burned is known with a relatively high degree of certainty. For the datum case configuration of Table I, the

surface area decreases 6.5% as the propellant burns. Heat loss to the chamber walls does not appreciably affect chamber pressure and temperature since the propellant insulates the walls. We propose to greatly reduce the complication associated with nonuniform ignition and with the uncertainties of the gas composition by using an igniter charge that consists of ultra-thin shavings (i.e., 5 to 15μ thick) of the main propellant. These shavings will loosely fill the chamber free volume and will be ignited by an electrically heated nichrome wire; flame will propagate quickly through the bed of shavings and provide an intense heat flux to the propellant surface. The rate at which the propellant shavings burn can be increased by pre-pressurizing the chamber. Heat flux from the ignition charge will be measured using an outer wall section instrumented with thin film calorimeters. The chamber will be fitted with a blow-out disk to limit the maximum pressure whenever limited-range pressure transducers are used to obtain very accurate pressure measurements at the lower pressures.

Figure 1b shows an alternate configuration in which the propellant configuration is a hollow cylinder which burns on the inner and outer cylindrical walls and the ends. The advantage of this configuration is that the propellant charge is easier to fabricate; the disadvantage is that the chamber walls are fully exposed and, thus, the heat loss will be greater.

ANALYSIS

The chamber pressure and mass generation responses (indicated in Fig.1c) will be calculated from a mathematical model whose primary components are coupled through numerical solutions to the energy equation for the propellant, the Zeldovich nonsteady heat feedback equations, the energy and continuity equations for the chamber, and a generalized form of the equation of state.

Burning Rate Dynamics

During ignition and rapid pressurization, two opposing effects in the combustion zone cause the instantaneous burning rate to differ greatly from the steady state burning rate corresponding to the instantaneous pressure, i.e., (1) the developing temperature profile in the condensed phase of the propellant and (2) the out-of-phase blowing effect of the reacting gases leaving the burning surface. The contributions of these effects are most easily explained in terms of an example which considers a rapid pressure increase from a low pressure condition. At the lower burning rate corresponding to the lower pressure prior to pressurization, the thermal wave is relatively thick. (Similarly, slow ignition produces a thermal wave thicker than the thermal wave corresponding to steady state burning.) As the pressure increases, the propellant surface layer is in effect preheated with respect to the thermal profiles at the higher pressures; the burning rate is enhanced while the preheated surface layer is being burned away. This enhanced burning rate causes the flame zone gases to have an enhanced velocity and, thus, the "blown" flame is thicker than the steady state flame corresponding to the instantaneous pressure. This blowing effect decreases the temperature gradient at the surface and the heat feedback from the flame. Thus, the burning rate of preheated propellant is moderated by the blowing effect when the burning rate exceeds the equilibrium burning rate. The interactions resulting from the rapid changes in pressure will also affect the flame temperature and chamber gas temperature. A primary objective of this study is to elucidate these dynamic processes.

In this development, the dynamic burning rate calculations employ the Zeldovich formulism (5) which offers the important advantage of considering the burning rate transients without having to understand the details of the flame and surface zone reactions. Since the methodology is covered thoroughly in Ref. 5, only the application is discussed in this paper.

The analysis and assumptions are discussed as they apply to highly loaded closed chambers. Because of the wide range of events and special purpose propellants that may be considered, the assumptions used in the analysis should be reviewed for each situation considered. The standard assumptions for application of the Zeldovich nonsteady heat feedback function are:

1. The rate processes in the flame zone adjacent to the surface (i.e., the fizz zone) and in the surface reaction zones can be considered quasi-steady in the sense that their characteristic times are short compared to the transition time of the pressure change. No such limitation is necessary for the thermal wave in the condensed phase.

2. No kinetic heat release occurs in the condensed phase below the surface reaction zone. Although the surface reactions occur in a zone of finite thickness, the zone is sufficiently thin that it can be considered as quasi-steady.

3. The condensed phase of the propellant is accurately represented as being homogeneous and isotropic.

4. Propellant combustion zones are not influenced by position and external forces such as shear forces from the flowing chamber gases.

The justifications for assumption 1 closely follow the arguments presented in Ref. 5. Thus following Ref. 5, the characteristic times for the condensed phase, surface zone, and gas phase are:

$$\tau_c = \alpha_c / r^2 \tag{1}$$

$$\tau_s = RT_s / E_s \tau_c \approx 0.1\ \tau_c \tag{2}$$

$$\tau_f = [\lambda_f c_p \rho_f / (\lambda_c c_f \rho_c)] \tau_c \approx 0.2 \times 10^{-3} p \tau_c \tag{3}$$

For the datum case conditions:

at $p = 100$ atm $\quad \tau_c \approx 0.0003$ sec and $\tau_f \approx 0.02\tau_c$ sec

$= 500$ $\quad \approx 0.00004$ and $\approx 0.1\tau_c$

Thus, over the pressure range of significant dynamic burning effects, the flame zone responds very quickly when compared to the response of the condensed phase temperature profile. Furthermore, the flame zone reacts quickly relative to the overall pressurization time (typically, 0.001 to 0.008 sec).

The energy equation for the condensed phase ($-\infty < x_c \leq 0$) has the following eigenvalue dependence on $T_c(0,t) = T_s(t)$

$$\rho_c c_c [\partial T_c/\partial t + r(T_s)\partial T_c/\partial x] = \lambda_c \partial^2 T_c/\partial x^2 \tag{4}$$

where under conditions of full ignition the burning rate r is related to the surface temperature through the pyrolysis law.

$$r = A_s \exp(-E_s/RT_s) \tag{5}$$

Note that surface temperature is dominated by the heat feedback from the flame. The initial condition for Eq. (4) is,

$$T(x) = T_0 \qquad \text{at} \qquad t = 0 \tag{6}$$

The first boundary condition is

$$T = T_0 \qquad \text{as} \qquad x \to -\infty \tag{7}$$

The second boundary condition is a series of conditions:

(1) heatup to ignition

$$\text{For } T_s < T_{ze}, \quad \lambda \frac{\partial T}{\partial x}\bigg)_{x=0} = q_{ig}(t) \tag{8}$$

(Until onset of surface regression, the temperature profile is calculated by a closed form heat conduction solution.)

(2) combined heating from ignition stimulus and from gas phase and surface reactions

$$\text{For } T_s \geq T_{ze} \text{ and } t < t_{ig}, \quad \lambda \frac{\partial T}{\partial x}\bigg)_{x=0} = q_{ig}(t) + \lambda_c \phi[r,p] \tag{9}$$

(3) burning during conditions of full ignition after the igniter burns out

$$\text{For } T_s \geq T_{ze} \text{ and } t \geq t_{ig}, \quad \lambda \frac{\partial T}{\partial x}\bigg)_{x=0} = \lambda_c \phi[r,p] \tag{10}$$

where ϕ is the Zeldovich heat feedback function developed in Ref. 5.

The result of the foregoing analysis of the propellant ignition and burning is one nonlinear, second order partial differential equation, [Eq. (4)] for $T(x,t)$, with a series of boundary conditions.

An expression for the dynamic flame temperature may be obtained under the following conditions: (1) the product composition in the flame zone and

the heats of reaction in the surface reaction zone and in the flame zone are not affected by the dynamic conditions, and (2) the specific heats in the surface reaction zone and the flame are equal. It follows from $\phi = (r/\alpha_c)(T_s - T_0)$ that the energy balance for both steady and unsteady states is:

$$r\rho_c \Delta h_f = \lambda_c \phi + r\rho_c c_c (T_f - T_s) \tag{11}$$

Therefore by considering a reference condition, the dynamic flame temperature is

$$T_f(\phi, r) = \frac{\lambda_c}{\rho_c c_{p,f}} \left[\left(\frac{\phi}{r} \right)_{ref} - \frac{\phi}{r} \right] - \frac{c_c}{c_{p,f}} \left[T_{s,ref} - T_s \right] + T_{f,ref} \tag{12}$$

Chamber Pressurization Dynamics

The analysis and assumptions are discussed as they apply to closed chambers in which the combustion gases are well stirred, i.e., thermal gradients within the chamber are not considered to be important. The assumptions for the closed chambers shown in Fig. 1 are:

1. Temperature and pressure variations can be accounted for by a lumped parameter treatment.

2. The flame zone gases are fully reacted when they enter the control volume which is adjacent to burning propellant surface.

3. Propellant surface ignites uniformly.

The condition of negligible total temperature and pressure gradients of assumption 1 is more justified for our small free volume chamber (defined by Fig. 1 and Table I) with a distributed propellant charge than for a large free volume chamber with the propellant charge at one end. In the former case, the combustion gases leaving the burning propellant surface are distributed along the length of the chamber and have velocity components (normal to the axis) which promote rapid mixing.

Assumption 2 is valid for nitrocellulose propellants at sufficiently high pressure that the dark zone thickness is small compared to the dimensions of the free volume surrounding the burning propellant. Establishing the validity of this assumption will have to await analysis of experimental data, since during the early phases of pressurization of high volumetric loading chambers reactions in the chamber may be significant.

The validity of assumption 3 depends on devising the experiment so that the interval of flame spreading through the propellant shavings is short compared to the total burning time of the main propellant charge.

The derivation of the chamber equations was carried out without specifying the gas law. During the numerical solution, gas properties are calculated as part of the finite difference solution (either from tabular data or from an equation of state and thermodynamic relationships) for each set of calculated pressure, p_{ch}, and temperature, T_{ch}. The initial

conditions are

$$r = 0$$

$$p_{ch} = p_{init}$$

$$T_{ch} = T_{init} \tag{13}$$

The mass continuity equation for the free volume in the chamber (see chamber control volume in Fig. 1a) is

$$d(\rho_{ch} V_{ch})/dt = m_b + m_{ig} \tag{14}$$

where $m_b = \rho_c A_b(\tau_b) r$.

The chamber volume increase during burning is

$$dV_{ch}/dt = rA_b + m_{ig}/\rho_c \tag{15}$$

Following ignition, the burning surface area is a prescribed function of propellant geometry in terms of distance burned, τ_b.

The energy equation in the chamber is

$$\frac{de}{dt} = \frac{1}{\rho V_{ch}}[m_b(h_f - e) + m_{ig}(h_{ig} - e) - Q_{loss}] \tag{16}$$

For M-6 propellant a simpler form of the energy equation can be used with very little loss in accuracy since h_f, c_v and $\partial h/\partial T)_p$ vary slightly (see Table II) and, as shown in Fig. 2, the Noble-Abel equation of state is an excellent approximation. Accordingly, $de \approx c_v dT$, and

$$\frac{dT}{dt} = \frac{1}{c_v \rho V_{ch}}[m_b(c_p T_f - c_v T) + m_{ig}(c_p T_{ig} - c_v T) - Q_{loss}] \tag{17}$$

The generalized equation of state $\rho = p/T\omega(p,T)$ is expressed in differential form (and then combined algebraically with Eq. 14):

$$\frac{d\rho}{dt} = \frac{1}{\omega T}\frac{dp}{dt} - \frac{p}{\omega T^2}\frac{dT}{dt} - \frac{p}{T\omega^2}\frac{d\omega}{dt} \tag{18}$$

In the numerical solution, $\omega(p,T)$ may be input in tabular form and particular values of $\omega(p,T)$ are found by a two point interpretation.

The heat loss from the chamber gases to the chamber walls are approximated by treating the chamber wall as several thermally thick surfaces that are heated by a combination of radiation and convection

$$Q_{loss} = \sum_1^n A_{w,n}\left[h_n\left(T_{ch} - T_{w,n}\right) + \sigma A_{1-2}\left(T_{ch}^4 - T_{w,n}^4\right)\right] \tag{19}$$

The wall temperatures are calculated by integral solutions to the heat conduction equation [for discussion of Eq. (20) see Ref. 6]

$$T_{w,n} = \frac{4\alpha_w}{3\lambda_w^2} \int_0^t \frac{q_w^2 (T_{ch} - T_w)}{(T_w - T_0)(2T_{ch} - T_w - T_0)} \, dt \tag{20}$$

Equation (20) was obtained by substituting a third order temperature profile into the heat conduction equation with a convective boundary condition and setting up the indicated integration.

As the igniter gases pass over the unignited propellant, they give up heat. As a result, the igniter gas temperature as it mixes with the chamber gases is considered to be

$$T_{ig} = T_{ig,ref} - A_b q_{ig} / (c_p m_{ig}) \tag{21}$$

The primary result of the foregoing analysis of the chamber and propellant burning conditions is a coupled set of three nonlinear, first order ordinary differential equations (Eq. 14, 15, and 17) for p_{ch}, T_{ch}, and V_{ch} and one nonlinear, second order partial differential equation, i.e., the energy equation for the condensed phase, Eq. (4). The energy equation for the condensed phase along with its boundary conditions was solved using the methods of explicit finite differences. Equations (14), (15), and (17) were solved by a predictor-corrector technique employing a variable time step.

CALCULATED RESULTS

A series of parametric studies were carried out for the closed chamber configuration shown in Fig. 1a loaded with M-6 (a single base nitrocellulose propellant). The datum case combustor conditions listed in Table I, were arrived at after using the analytical model to investigate a range of configurations. The M-6 condensed phase properties selected for the study are representative of typical nitrocellulose based propellant properties; a consistent set of property measurements for M-6 has yet to be accomplished. The combustion gas properties were calculated using the techniques of Ref. 7. As indicated in Table II, the ranges of M_w, $\partial h/\partial T)_p$, c_v and T_v are surprisingly small and, thus, mean property simplifications to the equations are soundly based. A similar series of thermochemical calculations for a double base propellant revealed that the ranges of these same variables are approximately twice as great. Figure 2 indicates that the large departures from ideal gas theory and that, in the range of interest, simple real gas laws (e.g., the Noble-Abel equation) can adequately describe the gas properties.

Burning rate, chamber temperature, and pressure during the operating sequence of the datum case are shown on Fig. 3a. After the propellant ignites, the heat flux from the ignition charge produces a burning rate overshoot since it is the same order of magnitude as heat feedback from the propellant flame. The second overshoot in burning rate is the increase in burning rate produced by the rapid increase in chamber pressure. Note that burning rate

and chamber temperature dynamics are very prominent during the first one-third of the burning interval. The short tail-off time of the igniter charge (i.e., 0.5 msec) produces the sharp demarkation between the burning rate overshoot produced by the igniter and the burning rate overshoot during the subsequent rapid pressurization; extending the tail-off time to 1.0 msec merges the two overshoots and there is no clearly distinguishable demarkation between the overdriven burning rate during ignition and during rapid pressurization (see the comparison on Fig. 3b).

The most widely used result from closed chamber experiments is dp/dt at prescribed pressures. Figure 4 shows the strong influence that loading density has on dp/dt. Figure 5 illustrates the application of a widely used parameter, relative quickness (RQ), to relate the dp/dt vs p results of closed chamber experiments. One of the more widely used definitions of relative quickness (RQ) states that dp/dt be recorded at four equally spaced values of pressure in the middle portion of the pressure-versus-time interval.(2) The dp/dt's are then compared to datum case or standard lot values at the four pressures in the following manner.

$$RQ = \frac{1}{4} \sum_{n=1}^{4} \frac{dp/dt}{dp/dt)_{datum}}\Bigg|_{p_n} \qquad (22)$$

For the four pressures indicated in Fig. 5b (i.e., $p_1 = 500$, $p_2 = 1000$, $p_3 = 1500$, and $p_4 = 2000$), RQ is referred to as $RQ_{0.5-2.0}$.

Figure 5 shows how changes in burning rate exponent (while keeping the burning rate at 68 atm constant) affect dp/dt and $RQ_{0.5-2.0}$. When considering the effects perturbing n, it must be realized that the values of RQ are very dependent on the pressure at which burning rate is held constant (i.e., the pivot point, p, on a ln r versus ln p plot). Indeed, as the pivot point pressure is increased toward the mean value of p_1, p_2, p_3 and p_4, $\partial RQ/\partial n$ becomes very small.

Figure 6 illustrates that the Eq. (22) definition of $RQ_{0.5-2.0}$ is totally blind to variations that greatly affect ignition and the initial pressurization phases. Even though decreasing the igniter heat flux and mass significantly alters the burning rate and chamber temperature responses before p = 300 atm, after p = 500 atm is achieved the changes in dp/dt vs p are not appreciable.

Figure 7 and Table III summarize the extent that changing propellant parameters, the closed chamber configuration, and the model affect the ignition and pressurization parameters. Based on the $RQ_{0.5-2.0}$ definition, variations in the burning rate coefficient and exponent have the greatest influence on RQ. To illustrate how dynamic response data can be obtained from closed chamber experiments, Table III includes $RQ_{0.05-0.2}$ calculations based on pressures at 50, 100, 150, and 200 atm. Note that these values of $RQ_{0.05-0.2}$ strongly reflect changes in dynamic response.

Figure 8 is a Zeldovich map which shows burning rate as a function of heat feedback to the condensed phase of the propellant. Following the Zeldovich formalism nonsteady burning rates can be related to steady state burning

rate changes that correspond to changes in the propellant's initial temperature. A detailed discussion of this relationship is given in Ref. 5. The locus of burning rates illustrate the relationships between burning rate overshoot and increases in initial temperature. For example, the $r/r_{eq} \approx 2$ overshoot following ignition (see Fig. 2) corresponds to the increase in steady state burning rate obtained by increasing the initial temperature of the propellant from 298 to approximately 480 K. As the dynamic effects diminish, the locus of burning rates merges with the burning rates corresponding to $T_0 = 298$ K.

Several recent efforts have attempted to develop empirical dynamic burning relationships in terms of dp/dt and other instantaneous parameters. One such relationship originated with von Elbe (6) and has been extended by others (e.g., Refs. 1 and 9). To date none of these empirical relationships successfully compared with the more complete dynamic burning rate models.(5,10) Two of the several reasons for this are (1) if the method of Ref. 6 is used, the essential features of the condensed phase temperature history are lost since the computational scheme uses a series of steady state temperature profiles in the condensed phase, and (2) the method does not consider the dynamic coupling between the heat feedback from the flame zone and the propellant surface conditions (i.e., the relationship indicated in Eq. 10). Two examples of the lack of effectiveness of the empirical models are shown in Fig. 9. If the empirical relationships are to be useful, an approximate one-to-one relationship between r/r_{eq} and some dp/dt parameter must be found. The left-hand figure shows that input parameters that influence the dynamic response greatly alter the relationship between r/r_{eq} and $(a_c/r_{eq}^2)(d \ln p/dt)$. Proponents of the empirical dynamic relationship may counter that since changing σ_p changes the propellant, the dynamic burning relationship will change also. However, in the right-hand figure, the propellant parameters are the same for all three cases, but ignition and pressurization responses have been altered. Note that r/r_{eq} is very dependent on the particular ignition and pressurization response and is not specified (even approximately) by the parameter $(a_c/r_{eq}^2)(d \ln p/dt)$. Attempts to correlate other dp/dt parameters were unsuccessful. Thus the burden of demonstrating that a particular empirical dynamic burning rate equation is a good approximate is on the users of the equation. In the meantime, there is no justification for using empirical dynamic burning rate equations to calculate specific burning rate responses.

CONCLUSIONS

An analytical model has been developed that considers the complete thermodynamic sequence in the closed chamber configuration that is being proposed for future studies of dynamic responses. The model goes far beyond previous efforts to simulate closed chambers since it combines for the first time the following features:

1. Heat up to ignition.
2. Dynamic burning rate and flame temperature based on transient development of the propellant temperature profile.
3. A generalized treatment of real gas effects.
4. Heat loss to the chamber walls.
5. Chamber wall temperature calculated as a function of time.
6. The chamber temperature based on a solution to the energy equation.

Based on the analytical results, the operability and the Table I dimensions for the closed chamber shown in Fig. 1a appear to be realistic. Efforts are proceeding to obtain data using the device and to explain the data in terms of the model.

Present methods of measuring relative quickness exclude the contribution of ignition and early stage pressurization events which are known to be the precursors to serious overpressures and velocity dispersions produced by improperly designed large caliber propelling charges. Accordingly, whenever dynamic response information is sought, careful attention must be given to the early portion of the p versus t trace. The routine quality control type of RQ's are totally blind to dynamic response irregularities since they use data from the well behaved middle portion of the dp/dt versus p trace.

For systems with smooth, well behaved pressure versus time characteristics, the routine quality control type of RQ (based on the middle portion of the dp/dt versus p trace) is of value in establishing charge weight. Under such conditions, this study shows that variations in the coefficient and exponent of the burning rate equation influence RQ most strongly and that the assumptions of no heat loss, Noble-Abel equation of state, no dynamic burning, and ignoring the details of the ignition processes have little influence on the calculated RQ values taken from the middle of the dp/dt versus p trace.

ACKNOWLEDGMENT

The authors appreciate the contributions of Dr. Eli Freedman of the Ballistic Research Laboratories who carried out the thermochemistry calculations and advised them concerning the proper treatment of real gas effects.

REFERENCES

1. Krier, H. and Shimpi, S. A., "Predicting Uniform Gun Interior Ballistics: Part 1 - An Analysis of Closed-Bomb Testing." Technical Report AAE 74-5, July 1974, Univ. of Illinois, Urbana-Champaign, Ill.

2. Fitzsimmons, F. J., "Concept Scope of Work for PEMA Project 5774186 Acceptance of Propellant Via the Continuous Process (Project Autocap)," Report No. ASRSD-QA-A-P-55-73, Dec. 1972, Product Assurance Directorate, Picatinny Arsenal, Dover, N.J.

3. Sandow, J., "High Pressure Combustion Study of a Double-Base Propellant," Technical Memorandum No. 1953, June 1970, Feltman Research Laboratories, Picatinny Arsenal, Dover, N.J.

4. May, I. W., Clarke, E. V. and Hassmann, H., "A Case History: Gun Ignition Related Problems and Solutions for the XM-198 Howitzer." Interim Memorandum Report No. 150, Oct. 1973, U.S. Army Ballistic Research Laboratories, Aberdeen Proving Ground, Md. Also "Subtle Effects of Low Amplitude Pressure Wave Dynamics on the Ballistic Performance of Guns," to appear in the Proceedings of the 11th JANNAF Combustion Conference, 1974.

5. Summerfield, M., Caveny, L. H., Battista, R. A., Kubota, N., Gostintsev, Yu. A. and Isoda, H., "Theory of Dynamic Extinguishment of Solid Propellants with Special Reference to Non-Steady Heat Feedback Law," Journal of Spacecraft and Rockets, Vol. 8, No. 3, March 1971, pp. 251-58.

6. Peretz, A., Kuo, K. K., Caveny, L. H. and Summerfield, M., "The Starting Transient of Solid-Propellant Rocket Motors with High Internal Gas Velocities," AIAA Journal, Dec. 1973, pp. 1719-1727.

7. Freedman, Eli, "A Brief Users' Guide for the Blake Program." Interim Memorandum Report No. 249, July 1974, Ballistic Research Laboratories, Aberdeen Proving Ground, Md.

8. Von Elbe, G. and McHale, E. T., "Extinguishment of Solid Propellants by Rapid Depressurization," AIAA Journal, Vol. 6, No. 7, pp. 1417-1419, July 1968.

9. Osborn, J. R. "Evaluation of Solid Propellant Ballistic Properties," Combustion and Flame, Vol. 20, 1973, pp. 193-197.

10. Krier, H., T'ien, J. S., Sirignano, W. A. and Summerfield, M., "Nonsteady Burning Phenomena of Solid Propellants: Theory and Experiments," AIAA Journal, Vol. 6, Feb. 1968, pp. 278-285.

Nomenclature

a	burning rate law coefficient for empirical relation ap^n	
A_b	propellant burning surface	cm^2
A_s	pre-exponential factor in pyrolysis law	cm/sec
A_{1-2}	overall interchange factor for radiation between gas and region being heated	
c	specific heat	cal/g-K
c_p	specific heat of combustion gases at constant pressure	cal/g-K
c_v	specific heat of combustion gases at constant volume	cal/g-K
E_s	activation energy in pyrolysis law	cal/g-mole
h	enthalpy	cal/g
h	convective heat transfer coefficient	cal/cm^2-sec-K
Δh_f	net heat release during propellant combustion	cal/g
m	mass flow rate	g/sec
M_w	average molecular weight	g/g-mole
n	exponent of ap^n burning rate law	
p	pressure	atm, MPa
q_{ig}	heat flux from ignition stimulus	cal/cm^2-sec
R	universal gas constant	cal/g-mole-K
RQ	relative quickness (see discussion of Eq. 22)	
r	burning rate	cm/sec
t	time	sec
T	temperature	K
T_0	initial temperature of propellant	K
T_{ze}	threshold surface temperature for first flame	K
V_{ch}	chamber volume	cm^3,
x	distance	cm
α	thermal diffusivity	cm^2/sec
λ	thermal conductivity	cal/cm-K-sec
ρ	density	g/cm^3
ϕ	temperature gradient at interface between surface reaction zone and non-reacting condensed phase	K/cm
σ	Stefan-Boltzmann constant	
σ_p	temperature sensitivity of burning rate at constant pressure $(\partial \ln r/\partial T_0)_p$	K^{-1}
η	covolume in Noble Abel equation of state	cm^3/g

τ	characteristic time	sec
τ_b	thickness of propellant burned	cm
μ	main and igniter propellant loading density in chamber	g/cm^3

Subscripts

b	burning propellant
c	condensed phase
ch	chamber conditions
eq	steady state condition which corresponds to instantaneous pressure
f	flame condition, flame zone
ideal	perfect gas
init	initial; condition of a controlled environment
ig	igniter
p	constant pressure
prop	propellant
ref	reference conditions: p = 68.08 atm (6.90 MPa), T_0 = 298 K
s	surface reaction zone
v	constant volume
w	wall
ze	temperature of flame development
0	ambient condition of unburned propellant

Table I

Combustor Conditions For Datum Case

Loading Density, $\mu = 0.2$ g/cm^3
Grain Configuration: rod and tube
Length = 3.00 cm
Chamber ID = 3.000 cm
Rod OD = 1.411 cm
Web Thickness = 0.050 cm
Chamber Volume: 14.47 to 16.45 cm^3
Burning Area: 43.05 to 40.26 cm^2
Igniter Burning Time: 1.0 msec plus 0.50 msec tail-off
Igniter Charge Mass = 0.0187 g
Heat Flux from Igniter = 200 cal/cm^2-sec
Propellant Mass = 3.284 g
Exposed Wall Surface = 11.0 cm^2
Chamber Material: Steel

Table II

Properties for M-6 Propellant as Used in Datum Case

COMBUSTION GASES: Range: 300-3300 atm and T = 2400 to 2800K

M_w = 23.28 g/g-mole	±0.086 (± 0.4%)	RANGE
$(\partial h/\partial T)_p$ = 0.444 cal/g-K	±0.012 (± 2.7%)	RANGE
c_v = 0.349 cal/g-K	±0.017 (± 4.9%)	RANGE

pv/nRT in tabular form ranges from 1.033 to 1.402

T_v = 2821 K ranges ±5K(± 0.2%) as loading ranges from 0.1 to 0.3 g/cm^3

CONDENSED PHASE:

$r = r_{ref}(p/p_{ref})^n$ cm/sec

where $n = 0.674$

r_{ref} = 1.448 cm/sec at 68.08 atm (6.90 MPa) and 298K

$\sigma_p = 0.0035\ K^{-1}$

E_s = 15,000 cal/g-mole

T_s = 623K at 1.448 cm/sec

$\lambda = 0.00073$ cal/cm-sec-K (± 0.00007)

$\rho = 1.58$ g/cm^3 (± 0.01)

$c = 0.37$ cal/g-K (± 0.03)

T_{ze} = 500K

Table III

Sensitivity of RQ to Datum Case Parameters

Variable Changed	Fractional Change $\Delta x/x$	$RQ_{0.5-2.0}$	$\frac{\Delta RQ}{\Delta x/x}$	$RQ_{0.05-0.2}$
n	+0.074	1.15	2.04	1.036
n	-0.074	0.87	1.78	0.965
n	+0.020	1.038	1.924	1.010
n	-0.021	0.963	1.860	0.991
a	+0.020	1.019	0.988	1.020
a	-0.020	0.979	1.023	0.978
μ, Loading density	+0.050	1.060	1.187	1.106
μ, Loading density	-0.050	0.941	1.173	0.948
σ_p	+0.143	1.001	0.005	1.048
σ_p	-0.143	0.999	0.004	0.989
m_{ig}, Igniter mass	-0.25	1.001	-0.008	1.005
q_{ig}, Igniter heat flux	-0.25	0.999	0.000	0.932
No heat loss to end wall	--	1.015	--	1.019
Noble-Abel Eqn. rather than $\omega(p,t)$	--	0.998	--	0.994
Increase igniter tail-off 0.005 sec	--	0.995	--	1.366
T_0	+0.02	1.027	1.351	1.040
c, Specific heat	-0.05	1.000	-0.007	1.038
λ, Thermal conductivity	+0.05	1.000	0.006	0.983

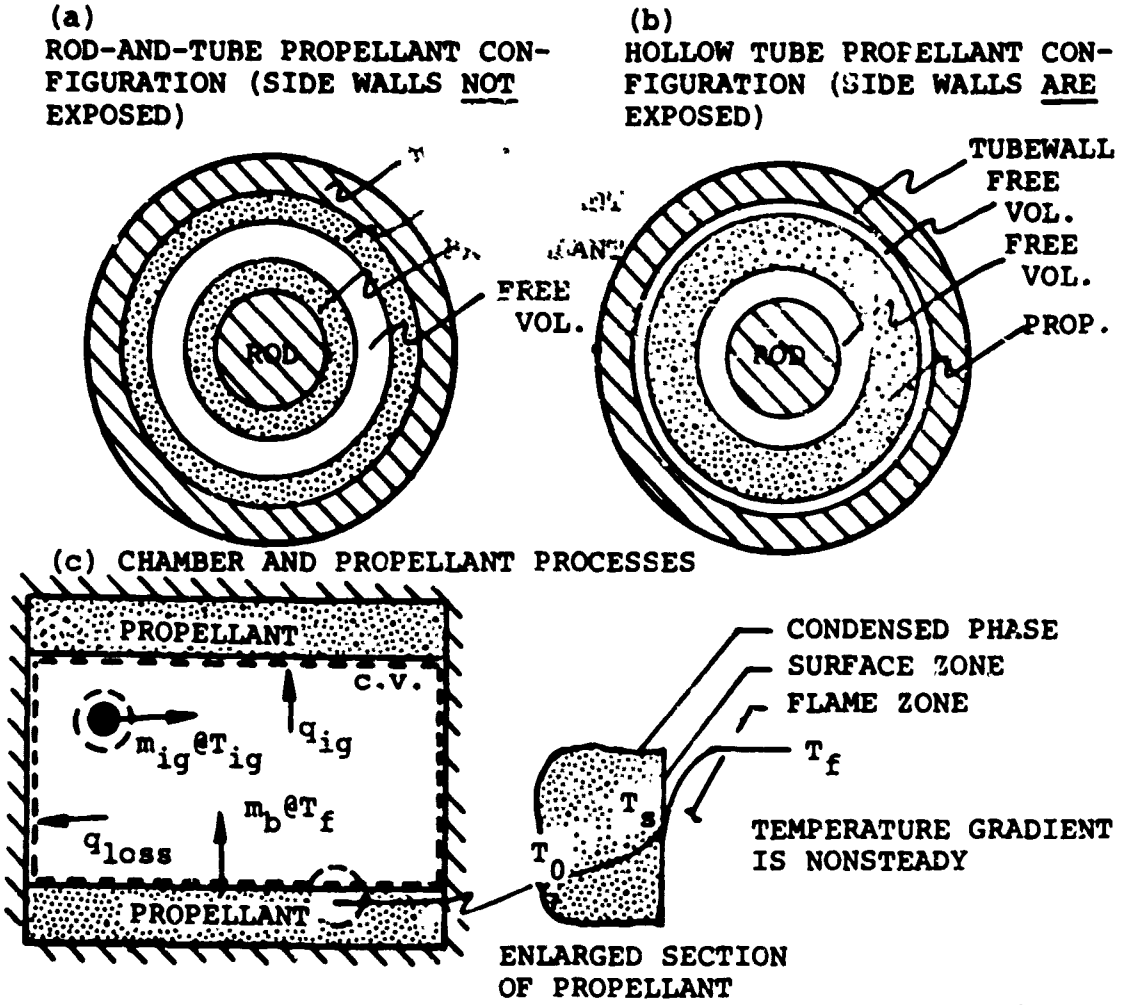

Fig. 1 Closed chamber configurations along with chamb and propellant processes considered in mathematical formulation.

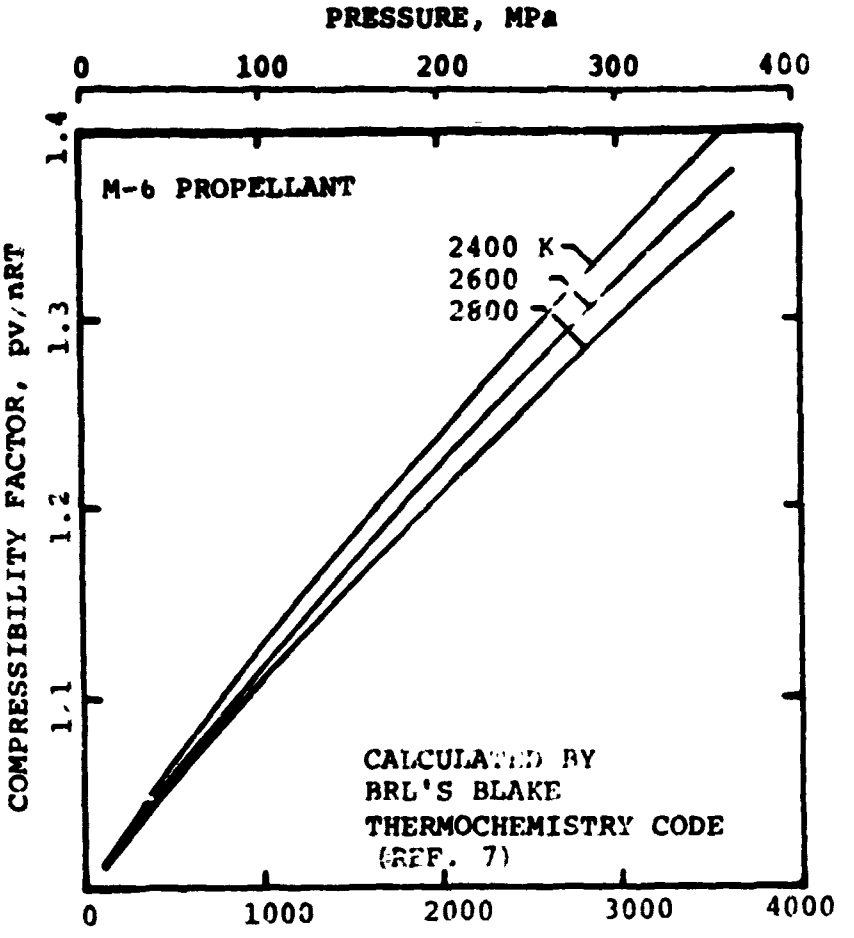

Fig. 2a Departure of M-6 propellant combustion gases from perfect gas theory in pressure and temperature range of closed chamber experiments. (Note: On the above plot the Noble-Abel equation of state produces a straight line with a slope of bM_w/RT, where b is the covolume. Thus, since on the above plot the isotherms can be approximated by such a straight line, the Noble-Abel equation describes the gases in the range of interest.)

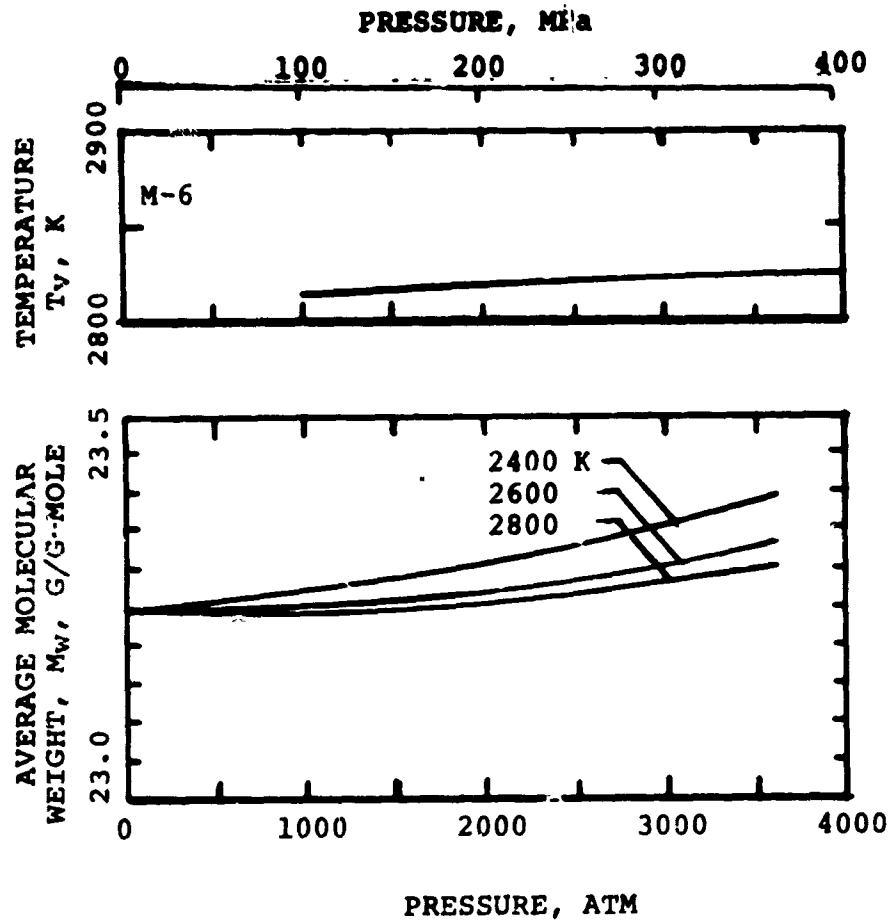

Fig. 2b Isochoric flame temperatures and molecular weights for M-6 propellant.

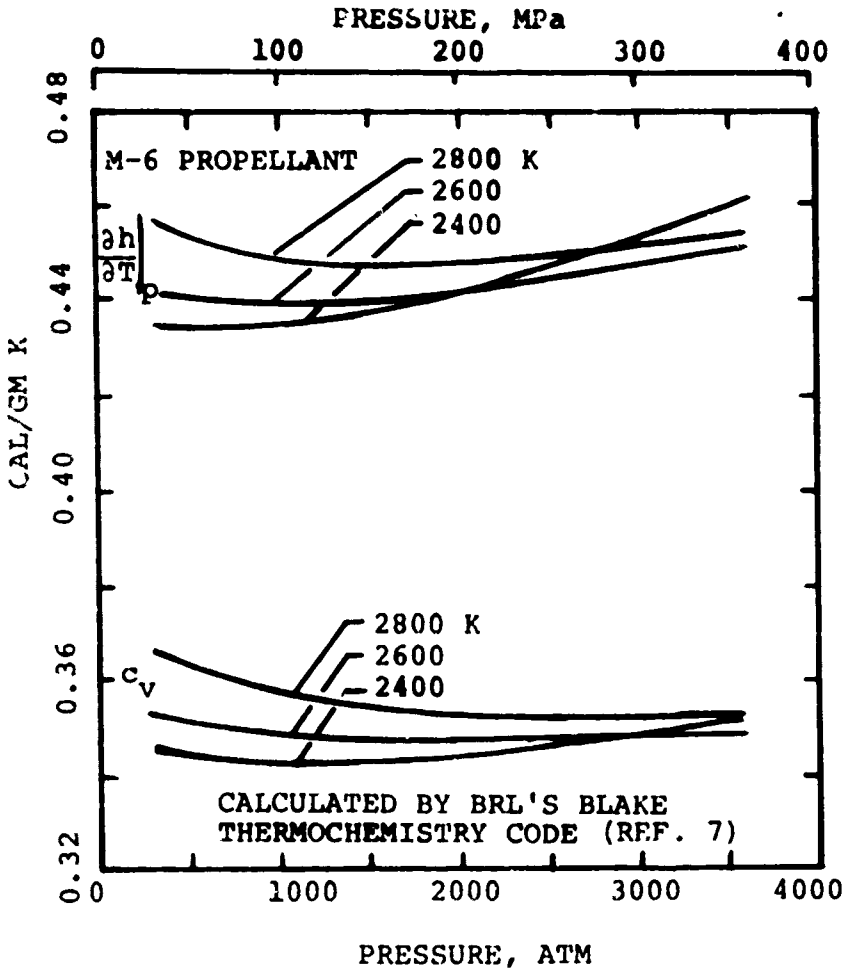

Fig. 2c Specific heats of M-6 propellants.

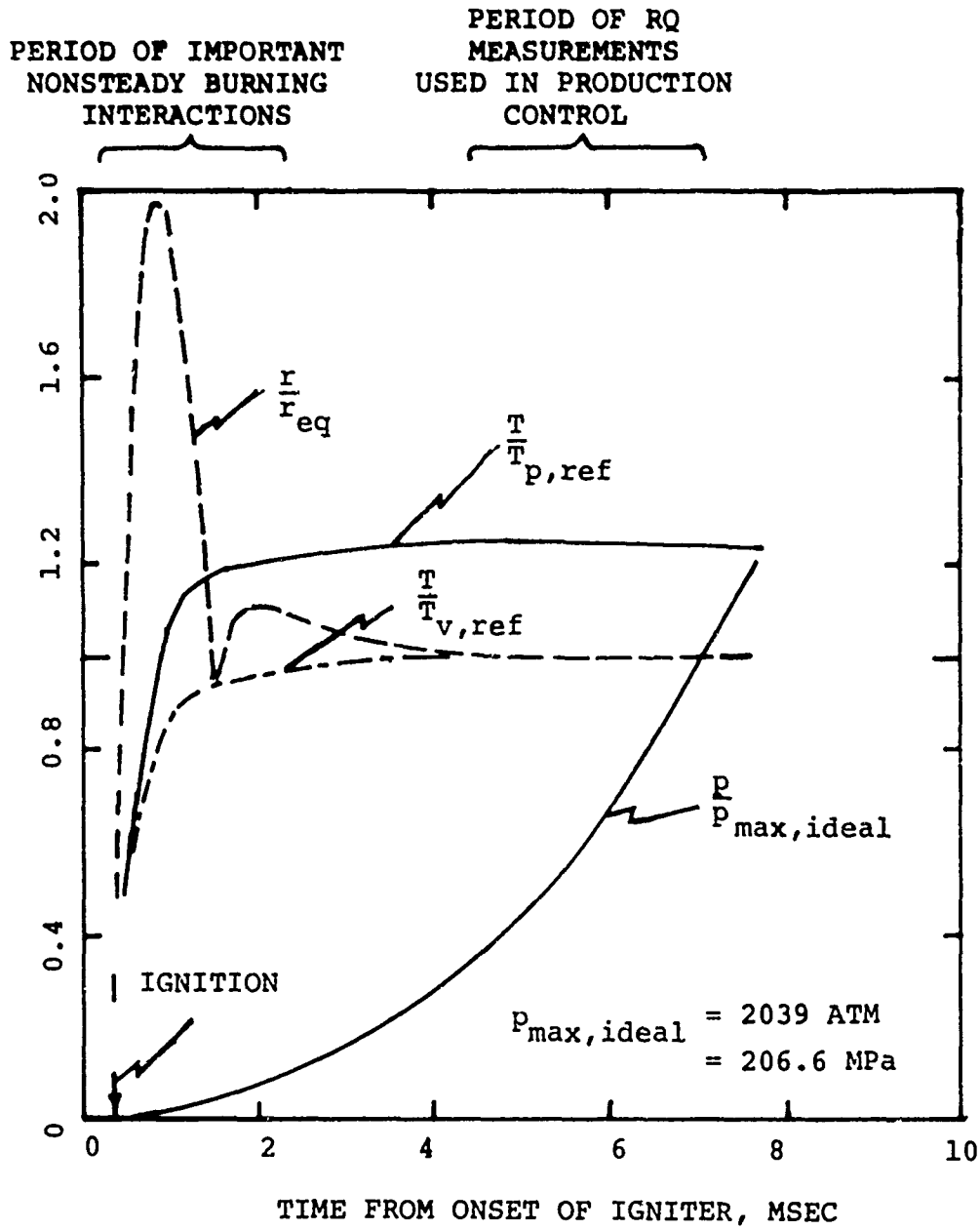

Fig. 3a Ignition and pressurization transients of datum case showing burning rate overshoots resulting from igniter and pressurization.

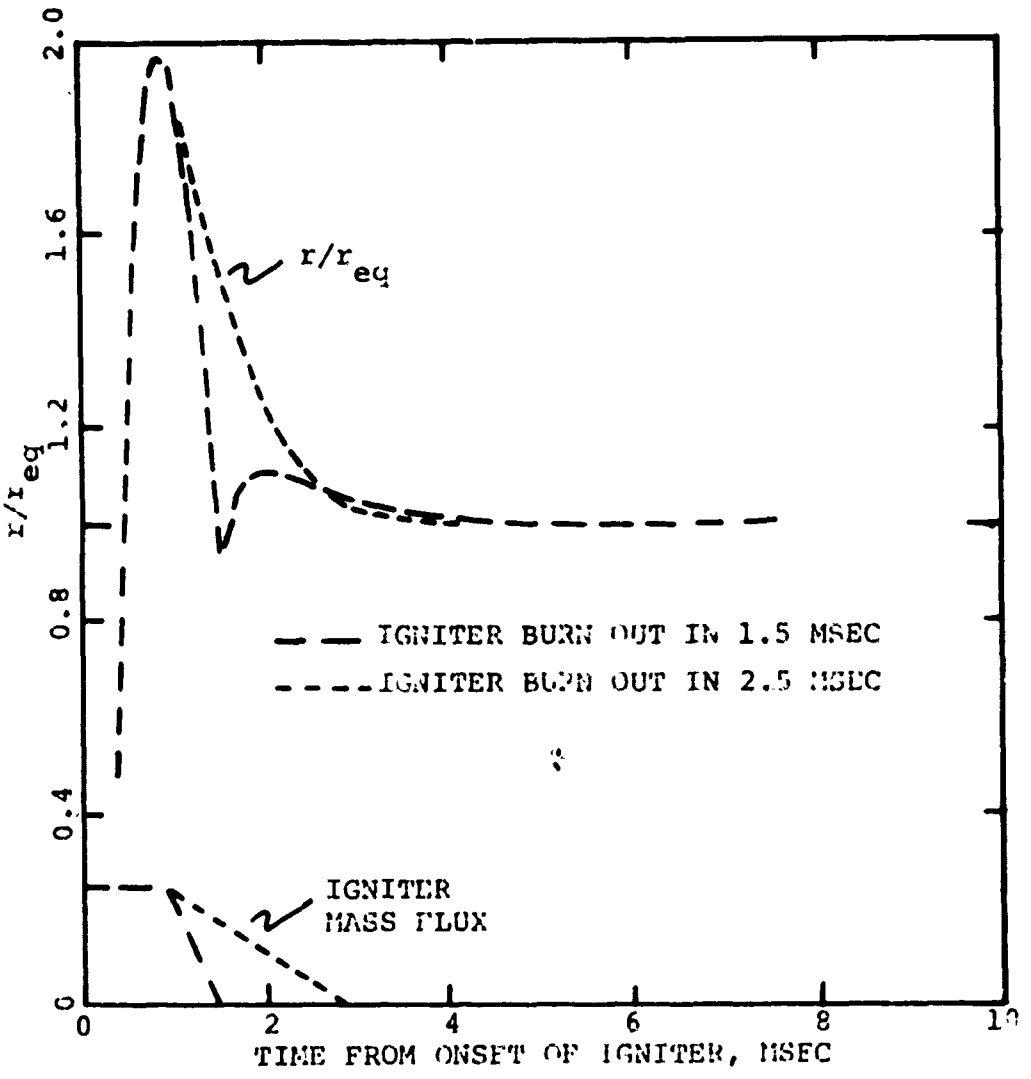

Fig. 3b Extending the action time of the igniter beyond the time of the burning rate overshoot associated with ignition preheating causes the two burning rate overshoots shown on Fig. 3a to merge.

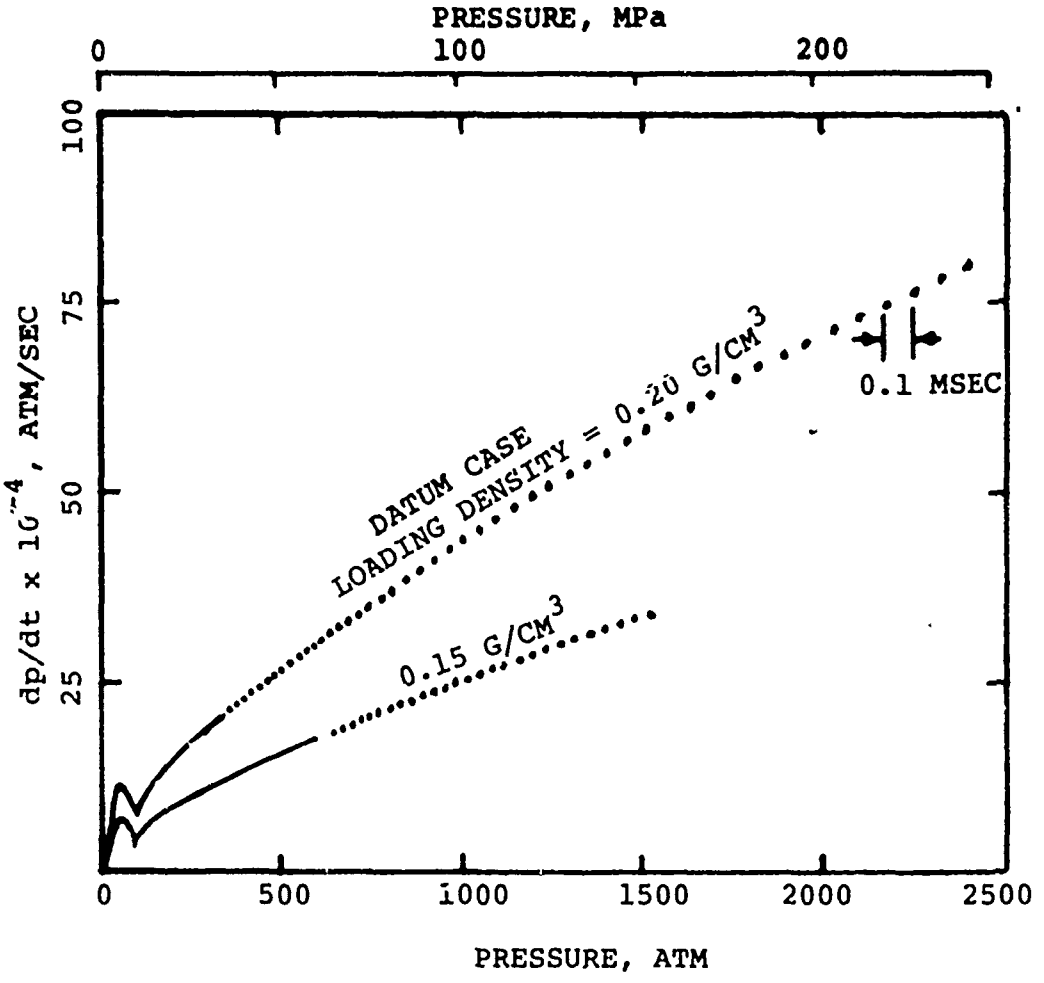

Fig. 4 Pressurization rate versus pressure showing effect of decreasing loading density.

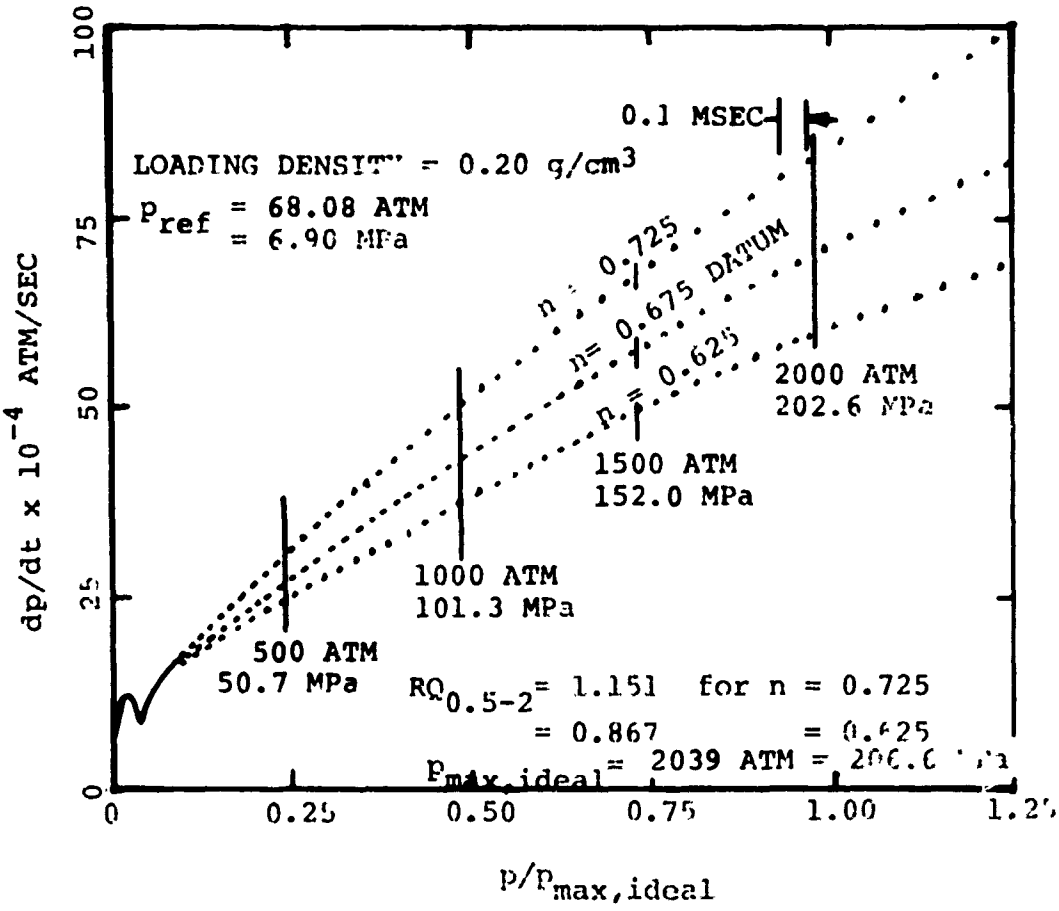

Fig. 5a Increasing relative quickness with increasing burning rate exponent. (Four pressures used in relative quickness calculation are indicated.)

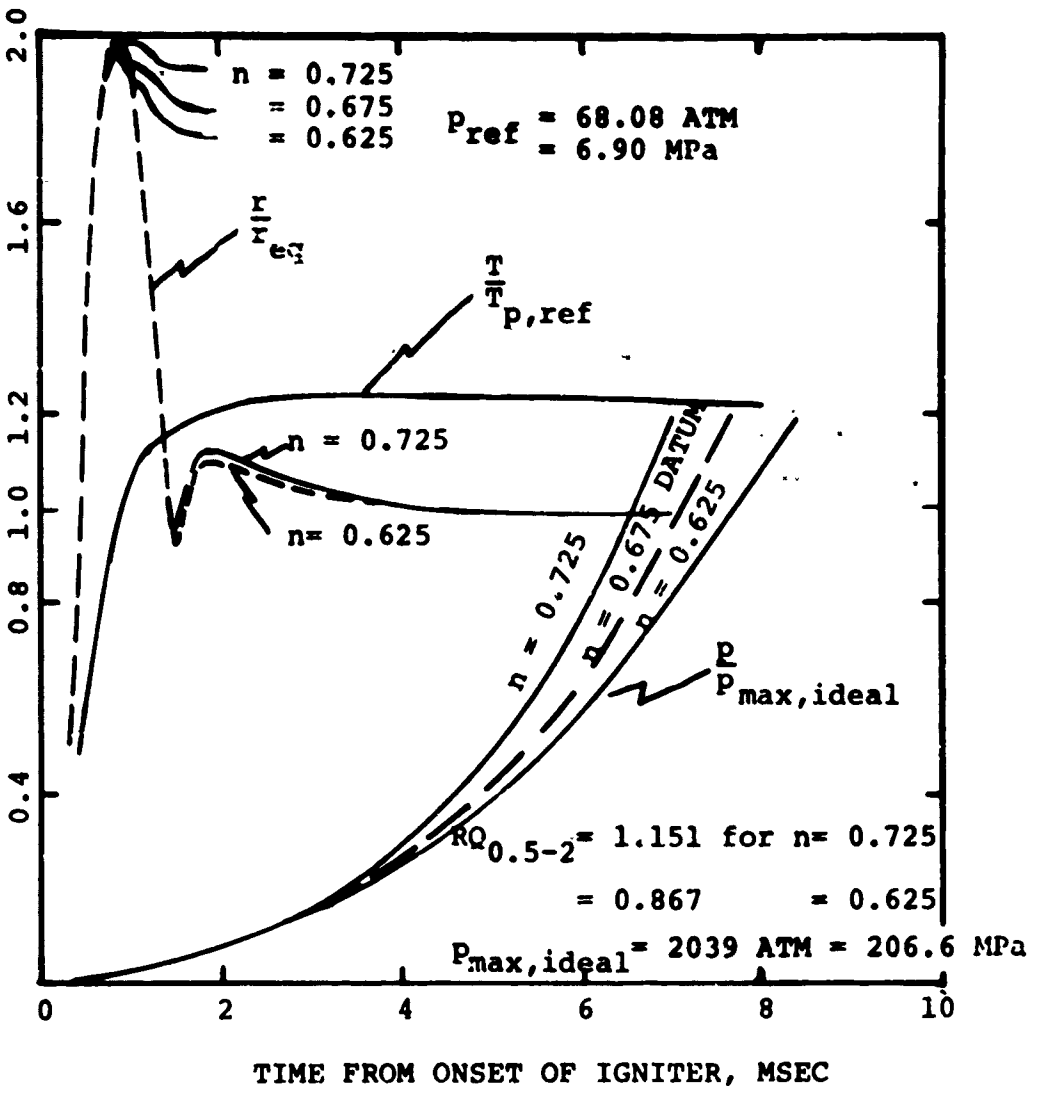

Fig. 5b Increasing pressurization rate with increasing burning rate exponent.

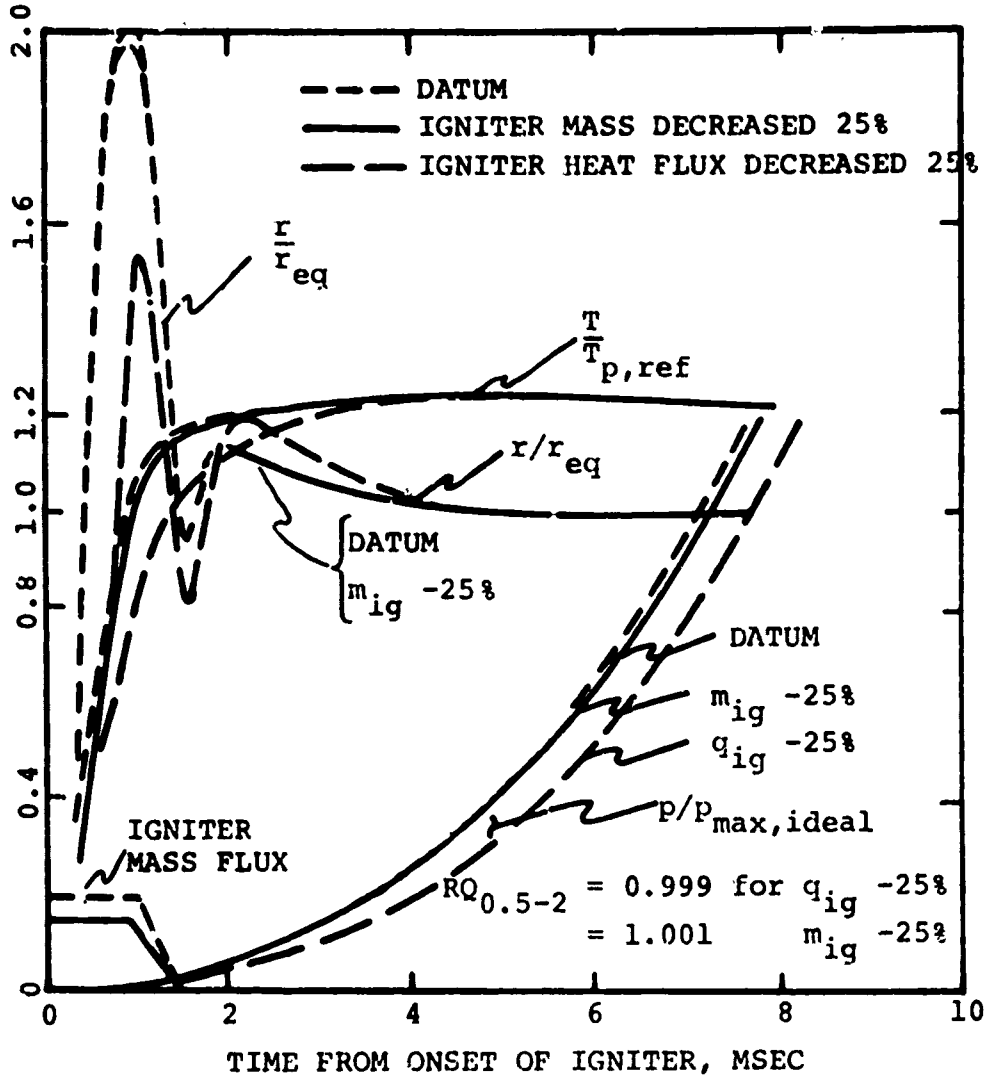

Fig. 6 Variations in igniter produce marked changes in the ignition transients but the shape of the latter portion of the p - t curve, and thus relative quickness, is not affected.

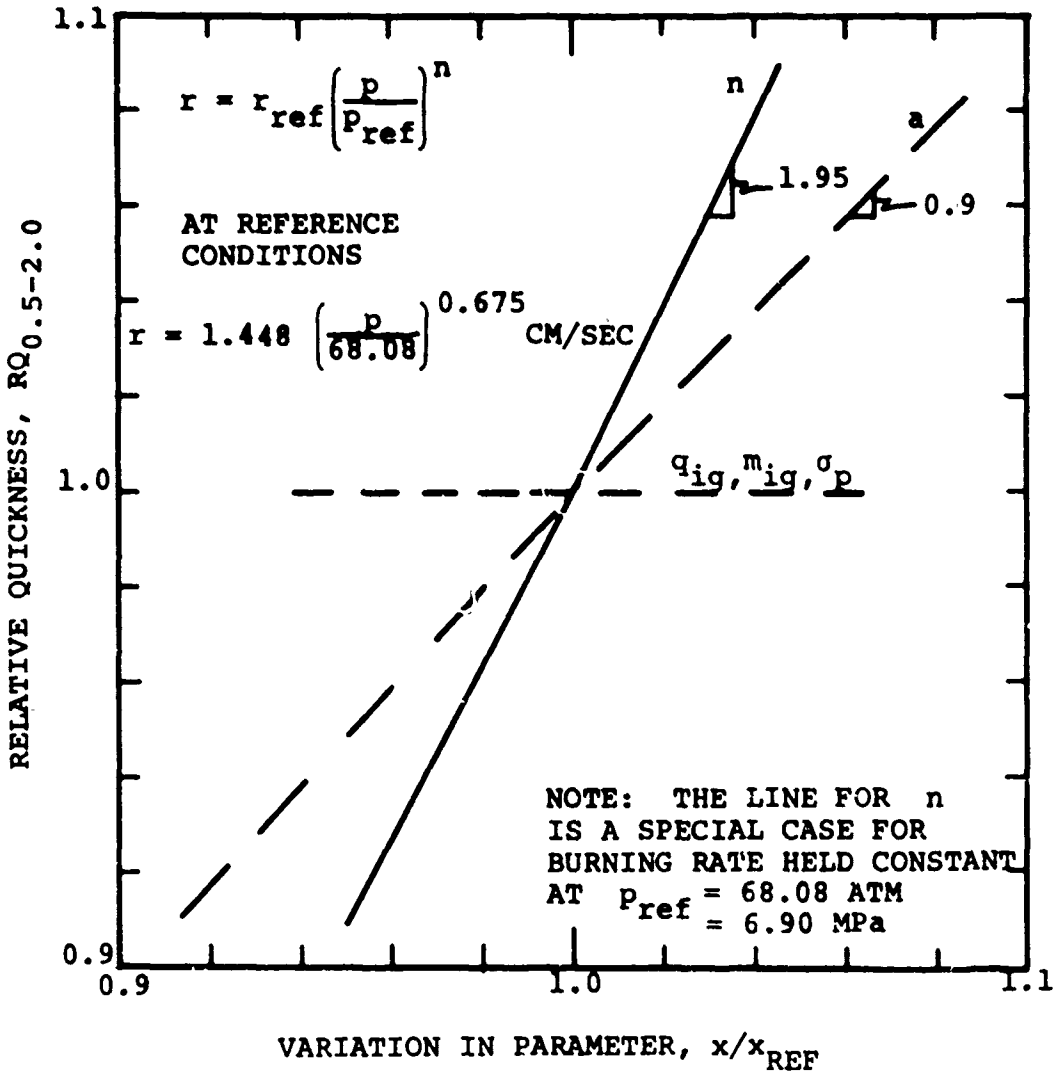

Fig. 7 Relative quickness variations in terms of ignition and propellant parameters.

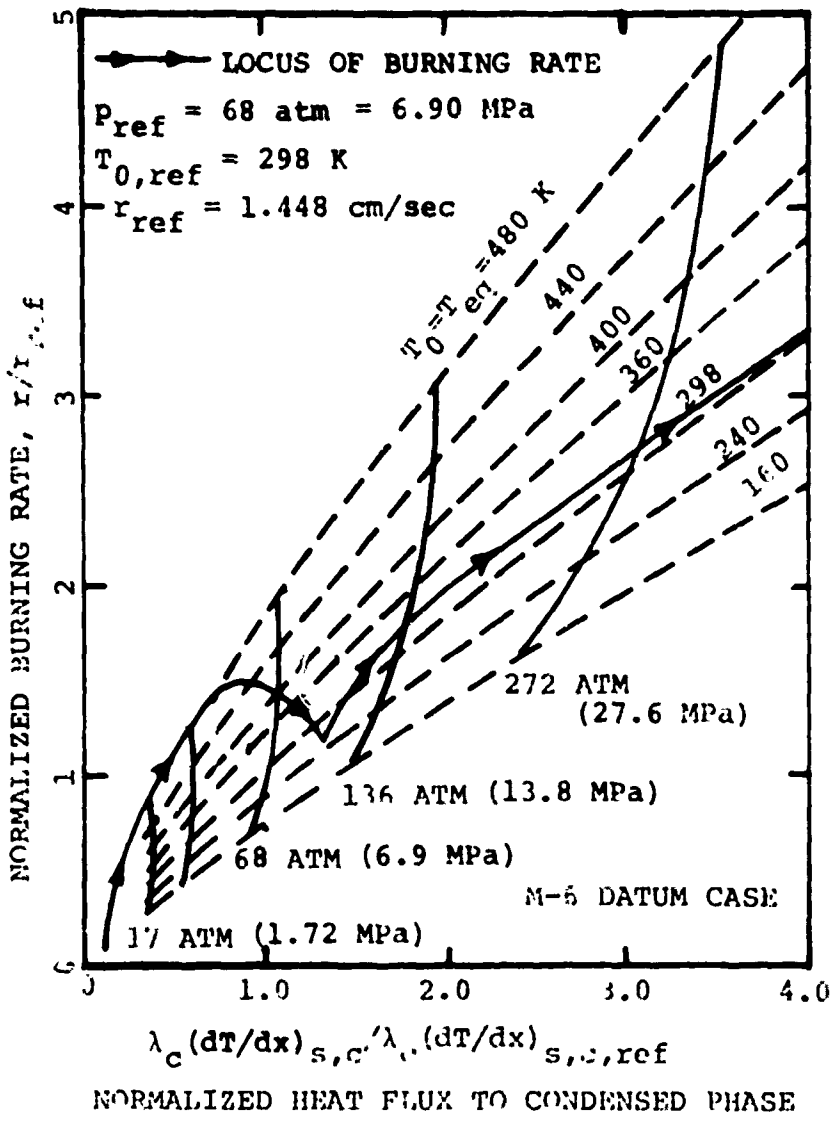

Fig. 8 Zeldovich map showing traverse of datum case.

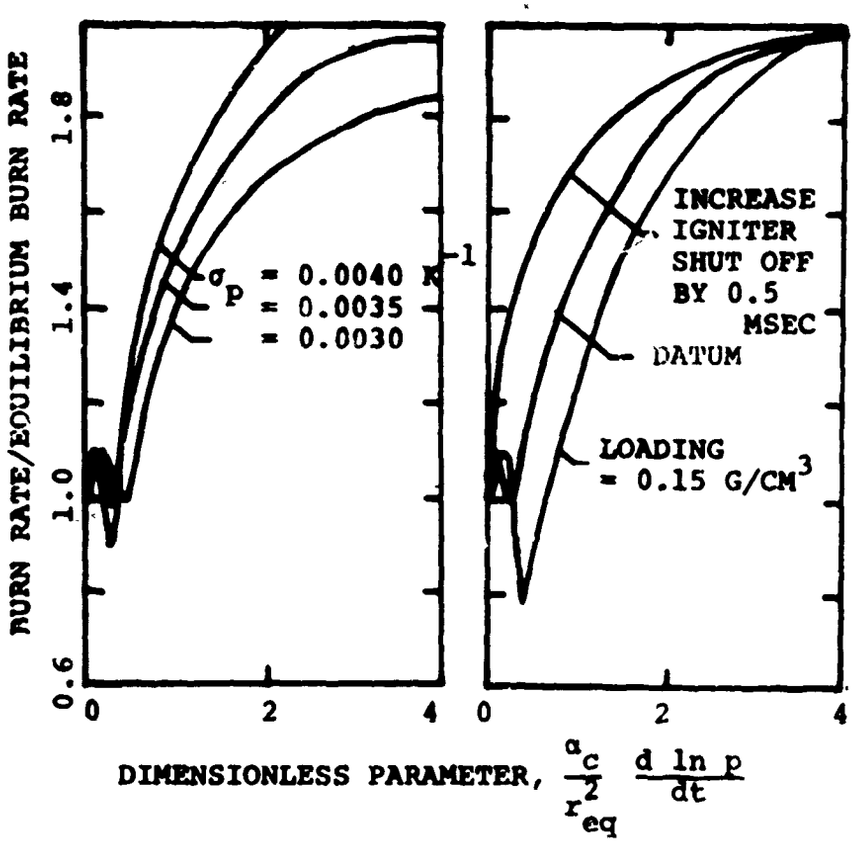

Fig. 9 Dynamic burning rates are not single valued with respect to a widely used dimensionless $\dot{p}$ parameter.